forests

MDPI

Article

Preparation of Superhydrophobic Wood Surfaces Modified Using MIL-88(Fe) via Solvothermal Method

Yu Han [1], Pingxuan Mu [2], Jinxin Wang [2,*] and Dawei Qi [2]

[1] College of Engineering and Technology, Northeast Forestry University, Harbin 150040, China; hanyu5214@nefu.edu.cn
[2] College of Science, Northeast Forestry University, Harbin 150040, China
* Correspondence: wangjinxin@nefu.edu.cn

Abstract: A superhydrophobic wood surface was produced by employing the solvothermal method to form shuttle-like, well-crystallized MIL-88(Fe) on the surface of wood and assembling a Octadecylphosphonic acid (OPA) reagent. The nanosized MIL-88(Fe) molecule caused the wood's surface to take on a nano mastoid shape. In addition, MIL-88(Fe) provides metal sites to capture OPA molecules, preventing the long-chain alkane hydrophobic group from contacting the surface of the wood. They both make a considerable difference in the growth of a hydrophobic wood surface. The results of the experiment indicate that the water contact angle (WCA) increases with reactant concentration. The WCA of the samples prepared with 5.0×10^{-2} M $FeCl_3$ was 140.57°. When the reactant concentration was 10.0×10^{-2} M, the greatest WCA = 153.69° reading was obtained. The research's findings present a novel technique for producing superhydrophobic wood surfaces.

Keywords: MIL-88(Fe); superhydrophobic; wood; solvothermal method

check for updates

Citation: Han, Y.; Mu, P.; Wang, J.; Qi, D. Preparation of Superhydrophobic Wood Surfaces Modified Using MIL-88(Fe) via Solvothermal Method. *Forests* **2023**, *14*, 1772. https://doi.org/10.3390/f14091772

Academic Editor: Milan Gaff

Received: 14 July 2023
Revised: 7 August 2023
Accepted: 17 August 2023
Published: 31 August 2023

1. Introduction

Wood, as one sort of natural material, is used in a variety of sectors, including flooring, furniture, and construction. However, the wood pieces develop deterioration, mildew, crazing, and deformation due to the wood's anisotropy, porosity, and many hydrophilic groups [1]. Therefore, it is essential to construct a hydrophobic wood substance. Scientists have come up with a sustainable way to create a highly compressible wood sponge-based sensor for human motion detection that is water-resistant and has a quick electrical reaction [2]. Additionally, functionalized wood surfaces have great thermal stability and dependability as well as effective solar-to-thermal energy conversion properties, all of which have significant applications in the development of advanced energy-related technologies and systems for thermal energy storage in moist or humid environments [3]. Numerous plant species naturally have very hydrophobic surfaces. The lotus leaf is a typical self-cleaning plant; when raindrops fall freely, they will wipe away any dust on the leaf [4]. According to studies, the lotus' superhydrophobic surface is mostly due to its nano mastoid structure and the presence of low surface energy epicuticular wax [5]. As proof, we thought that high nanostructure and low surface free energy should be taken into account while creating a superhydrophobic wood piece surface [6].

The surface area and roughness of the substrate have been modified over time using a variety of nanomaterials, including metal oxide nanoparticles [7–10], carbon materials [11], TiO_2 [12,13], SiO_2 [14], and ZnO [15,16]. However, only a few methods have been employed to manufacture these nanoparticles on organic materials; the majority were used on the surface of inorganic materials like glass, steel, or other inorganic materials. The majority of superhydrophobic wood pieces reported are produced by covering an oxide-particle combination (SiO_2 [17,18], Al_2O_3 [19]) with a material with a low surface free energy. This type of material adhesive power is weak, making the combination that is applied to the surface of wood pieces readily peel off. Therefore, several nanoparticles, such as

$CoFe_2O_4$ [7], ZnO [20], $Cu_2(OH)_3Cl$ [21], and TiO_2 [12], are synthesized on the surface of wood pieces, but their surface area is less than that of MOFs (metal–organic frameworks).

Additionally, the shape of these materials—round or flaky nanoparticles—makes it challenging to create huge mastoid structures. There is also minimal air between the particles and the wood pieces, which makes it simple for water molecules to link with the surface and adsorb into it [6].

MOFs are porous crystalline coordination polymer materials made up of networks of organic linkers and metal ions (or clusters). The unique micropore architecture contribute to high specific surface area and structural tunability, which give them numerous applications, including air purification, catalysis, drug delivery, and gas storage and separation [22–27]. However, as most of the MOFs are easily hydrolyzed, numerous techniques have been developed to create MOF-based superhydrophobic materials. These techniques include modifying MOFs with low surface free energy molecules [28,29], as well as doping metal ions [30]. However, it is still uncommon to find reports of superhydrophobic wood pieces that combine the benefits of MOFs with wood pieces. MIL-88(Fe) is one kind of MOFs, which has a shuttle-shaped morphology and exhibits high surface areas, large pore volumes, and good moisture and thermal stability [31,32].

Using the solvothermal process to create MIL-88(Fe) on the surface of wood pieces, which produces mastoid structures on the wood surface, exposes metal sites to collect low surface energy molecules, and provides a high surface area, superhydrophobic wood pieces were created based on the analysis mentioned above. The MIL-88(Fe) was modified using the low surface free energy n-Octadecylphosphonic acid (OPA). For the first time, the hydrophobic MOFs/wood composites were studied. MIL-88(Fe)'s shape and crystal structure were studied. It was made clear how the hydrophobic qualities may be improved. It will be interesting to apply wood pieces to specific applications, such as protecting it against decay, mildew, crack, and distortion, or used for oil–water separation, using the results to create superhydrophobic wood surfaces.

Based on the foregoing research, the advantages of poplar are that it grows quickly, has strong adaptability, wide distribution and is cheap. Superhydrophobic wood pieces were created via a solvothermal method coating MIL-88(Fe) on the poplar's surface, creating mastoid structures, exposing metal sites to collect low surface energy molecules, and producing a large surface area. The MIL-88(Fe) was modified using n-Octadecylphosphonic acid (OPA), which has a low surface free energy. MIL-88(Fe)'s crystal shape and structure were studied. The mechanism for enhancing hydrophobic characteristics was made clear. Because of the good mechanical performance and three-dimensional hierarchical and porous structure, as well as vertical channels of wood pieces, it is ideally suitable for liquid transport along the vertical channels [33]. It will be interesting to employ wood pieces for specific goals like oil–water separation. Additionally, the superhydrophobic layer can not only provide the wood pieces with waterproof, anti-fouling, self-cleaning functions, and avoid a variety of defects caused by water absorption of the wood, such as deformation, crack, decay, mildew, discoloration, and degradation, but it can also provide the wood with antibacterial, flame-retardant, conductive, magnetic, and microwave absorption properties, among other functions. It has significant scientific value as well as practical relevance for high-value-added wood use and functional development. These discoveries present a novel technique for producing superhydrophobic wood pieces.

2. Materials and Methods

2.1. Materials

Poplar lumbers (20 mm × 20 mm × 20 mm) were obtained from Harbin (Heilongjiang province, China), which were ultrasonically rinsed in ultrapure water and ethanol for 20 min, respectively, then dried at 100 °C for 24 h in a heating chamber. Iron chloride hexahydrate ($FeCl_3 \cdot 6H_2O$), N,N-Dimethylformamide (DMF), 1,4-dicarboxybenzene (H_2BDC), n-Octadecylphosphonic acid (OPA) and ethanol were purchased from Macklin Biochemical Co., Ltd. (Shanghai, China).

2.2. Preparation of MIL-88(Fe) Coated on the Wood Surface

The MIL-88(Fe)-modified wood pieces surface was prepared via a solvothermal process [34]. In a typical synthesis, different concentrations (0, 5.0×10^{-2}, 10.0×10^{-2} M) of $FeCl_3 \cdot 6H_2O$ and H_2BDC are used. The three distinct sample preparation procedures are the same, but various amounts of $FeCl_3 \cdot 6H_2O$ and H_2BDC are used, and the molar ratio of $FeCl_3 \cdot 6H_2O$ to H_2BDC is 1:1. As an example, take the sample at 5.0×10^{-2} M. In 30 mL of N,N-Dimethylformamide, completely dissolve 0.25 g of H_2BDC. Weigh 0.81 g $FeCl_3 \cdot 6H_2O$ and completely dissolve it in 30 mL of N,N-Dimethylformamide solution. The two solutions were added to the Teflon-lined stainless-steel autoclave (100 mL) and rapidly stirred for a further 30 min to ensure that they were well combined. This was carried out after the two solutions had been rapidly stirred for 20 min. The dry wood piece block was put into the mixture and, using the weight of the Teflon container with holes, it was placed above the wood pieces block so that it was completely submerged in the mixture. Since wood pieces has many pores, there is a lot of air in them, making it difficult for a solution to seep into the wood pieces. To remove the air in the wood pieces, a Teflon liner was placed in a vacuum vessel, vacuumed to 0.1 Mpa, with the pressure being held for 30 min; then, the vent was opened to let atmospheric pressure return. The process was repeated three times. The Teflon liner was put inside a stainless-steel reactor, sealed, and heated to 110 °C for 4 h in a blast drying oven and cooled down to room temperature naturally. Then, the wood block was taken out and put in an N,N-Dimethylformamide-filled container. After washing with stirring for 30 min, the unreacted terephthalic acid was be removed. The cleaning process was performed three times. To remove the DMF held in the MIL-88(Fe) micropores, the wood blocks were submerged in trichloromethane for 12 h. The samples were dried for 24 h at 103 °C in a vacuum-drying oven.

2.3. OPA@MIL-88(Fe) Coated Wood Surface

The wood pieces and as-prepared MIL-88(Fe)-coated wood pieces were subsequently modified using n-Octadecylphosphonic acid. The sample was immersed into 60 mL ethanol solution containing 0.15 g OPA for 3 h with stirring, and then kept it in vacuum tank at 0.1 Mpa for 1 h. The wood slice was washed with ethanol three times. Finally, the modified sample was dried at 103 °C via vacuum drying.

2.4. Characterizations

The surface morphology of the sample was analyzed via field emission scanning electron microscopy (SEM, Hitachi, SU8020), X-ray diffraction (XRD, Bruker, D8 ADVANCE, Japan), and a rotation anode X-ray diffractometer equipped with Cu Kα radiation (λ = 1.54178 Å) was employed in the determination of the crystal structure of samples. X-ray photoelectron spectroscopy (XPS) was performed using Thermo ESCALAB 250Xi, American with high-performance electron spectrometer using monochromatized Al Kα (hν = 1486.7 eV) as the excitation source to detect the chemical states of Fe and P elements. To evaluate the wettability of samples, OCA-50 (DataPhysics, Germany) was employed to measure water contact angle (WCA), with a distilled water droplet volume of 5 µL on each surface of wood pieces sample and a photo was taken after 10 s; then, another photo was taken until the water droplet shape was stable, and the WCA was fitted via Laplace–Young theory.

3. Results and Discussion

3.1. Surface Topography

The images captured using scanning electron microscopy (SEM) of clean wood pieces' surface coated in MIL-88(Fe) at various reactant concentrations are shown in Figure 1. Figure 1a depicts a perfectly smooth surface of wood pieces devoid of any particles to represent a perfect wood piece surface. After the solvothermal process, a sparse distribution of the particles was observed; they have an irregular form and a small, average grain size of 712.4 nm, as illustrated in Figure 1b. However, the dispersion is poor; extensive areas of

wood pieces that are not coated with MIL-88(Fe) are visible, and the crystal is small. This is due to the fact that the reactant concentration is insufficient for MIL-88(Fe) to grow with a high concentration on the surface of the wood pieces. In Figure 1c, there are numerous shuttle-like particles with an average length of 939.2 nm and a density distribution on the sample surface as the concentration rose. The characteristic morphology is almost the same as tat of the typical Fe-based MOF crystal, as previously reported [35]. The arrangement of the particles on the sample's surface provides Fe sites to capture OPA molecular to keep long-chain alkane hydrophobic groups from adhering to the wood's surface while simultaneously increasing surface area.

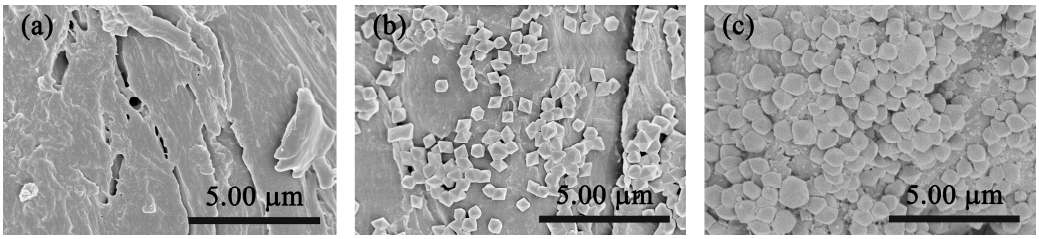

Figure 1. (**a**) SEM images of pristine wood pieces' surfaces, (**b**) MIL-88(Fe) coated on wood pieces surface solvothermal synthesized with 5.0×10^{-2} M reactant concentration, (**c**) with 10.0×10^{-2} M reactant concentration.

3.2. Crystal Structure

XRD was used to verify that the particles on the wood's surface are MIL-88(Fe) and to ensure that the sample is single-phase and free of impurities. In Figure 2, the XRD pattern is displayed. For pure poplar lumber, there are only two broad peaks for 2θ to 15.5° and 22.5°; these peaks represent the distinctive X-ray diffraction pattern of wood cellulose, which is one of the main constituents of poplar lumber [20]. Small peaks gradually appeared at 2θ to 9.2° and 10.3° in the pattern of wood pieces samples treated with 5.0×10^{-2} M and 10.0×10^{-2} M $FeCl_3 \cdot 6H_2O$, which can be attributed to (002) and (102) of MIL-88(Fe) (CCDC no. 647646). They steadily increased as the concentration of $FeCl_3 \cdot 6H_2O$ rose since they are so little that they are almost negligible at an MIL-88(Fe) concentration of 5.0×10^{-2} M. The MIL-88(Fe) particles are strongly crystalline, as demonstrated. At same time, as the reactant concentration rises, the crystallinity increased and more MIL-88(Fe) was produced on the wood's surface. These preliminary analyses indicate that the crystal particle on the wood surface is MIL-(88) without any impurities, the number of MIL-88(Fe) crystals increases with reactant concentration, which is consistent with SEM, and the OPA modification did not affect the instinct crystal structure of MIL-88(Fe).

3.3. Chemical States of Samples

To ensure that MIL-88(Fe) and OPA were properly coated on the surface of the wood pieces, the chemical states of Fe and P elements in MIL-88(Fe) and OPA-modified MIL-88(Fe) were determined via XPS in Figure 3. The peaks at around 711.5 and 724.8 eV are attributed to the Fe $2p_{3/2}$ and Fe $2p_{1/2}$, respectively, which is in good agreement with the report of MIL-88(Fe) [35]. As shown in Figure 3a, the binding energies of the Fe $2p_{3/2}$ and Fe $2p_{1/2}$ both show positive shifts since OPA was modified. This result further demonstrates the interaction between OPA and Fe atoms of clusters, resulting from the formation of Fe-O-P in OPA-modified MIL-88(Fe), which is supported by an earlier report [36,37]. Additionally, P 2p places the binding energy for OPA-modified MIL-88(Fe) at roughly 133.1 eV, while Figure 3b demonstrates that there are no noticeable peaks for MIL-88(Fe) wood pieces. This outcome shows that OPA successfully modified MIL-88(Fe), as seen by the presence of Fe sites on the surface of the wood pieces [38].

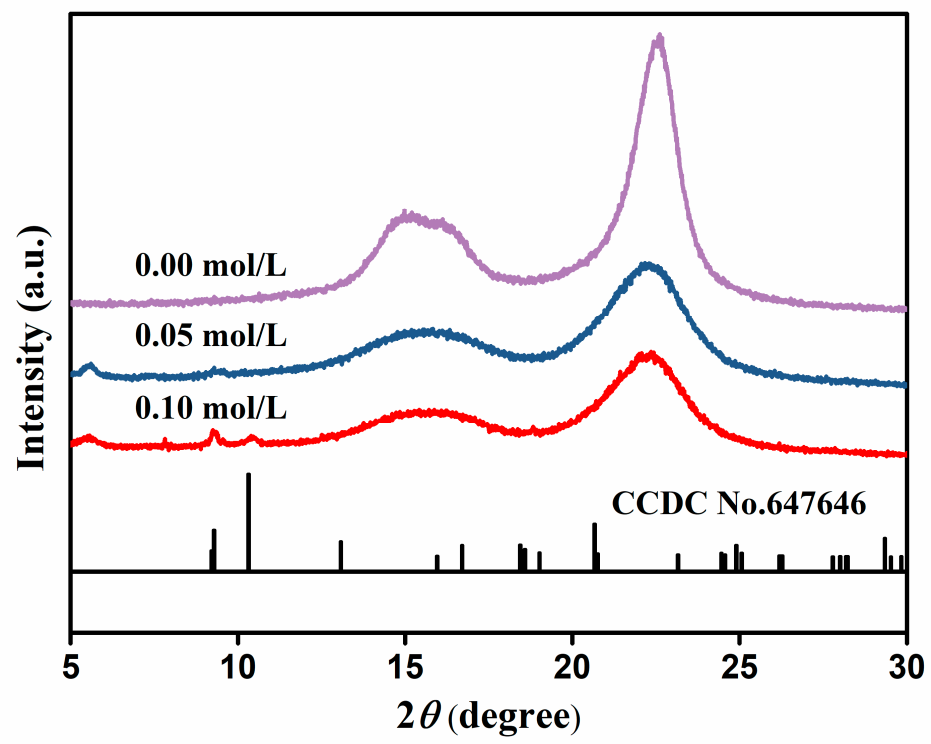

Figure 2. XRD patterns of the pristine wood surface and MIL-88(Fe) coated on wood surface solvothermal synthesized with 5.0 × 10^{-2} M, 10.0 × 10^{-2} M reactant concentration.

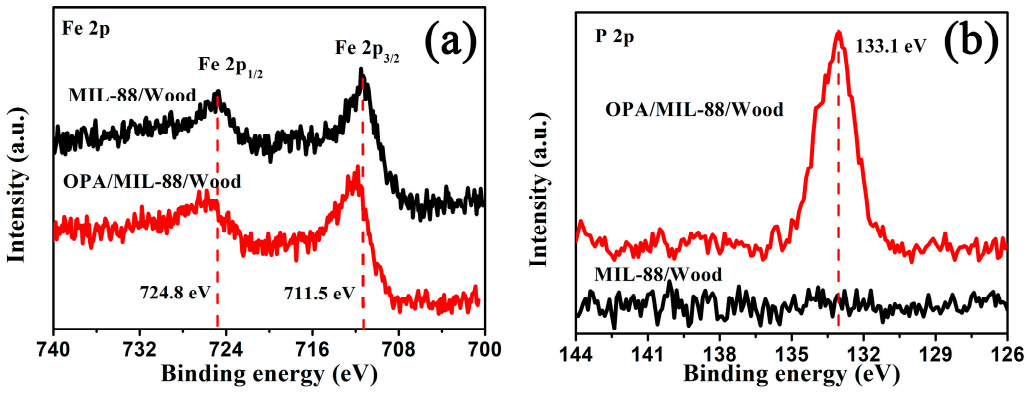

Figure 3. (**a**) Fe 2p XPS spectra of MIL-88(Fe)-coated wood pieces and OPA-modified MIL-88(Fe) coated wood pieces; (**b**) P 2p XPS spectra of MIL-88(Fe)-coated wood pieces and OPA-modified MIL-88(Fe) coated wood pieces.

3.4. Wettability of the Wood Pieces Surface

WCA measurements were used to assess surface wettability. Water (5 µL) was spilled on the wood piece surface unmodified with MIL-88(Fe) and held for 10 s before being photographed. Figure 4a depicts the shapes of the water droplets. The contact angle with the water was 137.8°. Because the poplar lumber was washed with ethanol and water under ultrasonication and then completely dried, this value is higher than in earlier reports [20]. Because the wood pieces had a lot of air, it was difficult for water to get in right away. However, because wood pieces are a hydrophilic material, water is absorbed fast into wood pieces. The contact angle was 122.2° until the water droplet shape was steady, as shown in Figure 4d. However, after 10 s, the WCA of the 5.0 × 10^{-2} M $FeCl_3$-treated wood surface reached 140.6°, as shown in Figure 4b, which was somewhat greater than that of unmodified wood pieces; however, when the shape of water was constant, the change in morphology of the water droplets was nearly undetectable, as illustrated in

Figure 4e, and reduced by almost 1 degree. More MIL-88(Fe) was synthesized on the wood surface to further raise the WCA of the material. The contact angle was 153.7°, as shown in Figure 4c, while the water droplet was left on the sample's surface for 10 s. As seen in Figure 4f, after holding for a sufficient amount of time, there was no discernible change in the WCA, and a 153.5° WCA was measured. The WCA is more than 150.0°, indicating that superhydrophobic wood pieces were created, according to the definition (WCA between 150.0° and 180.0°). The wood pieces were shielded from long-term water damage by the MIL-88(Fe) coating.

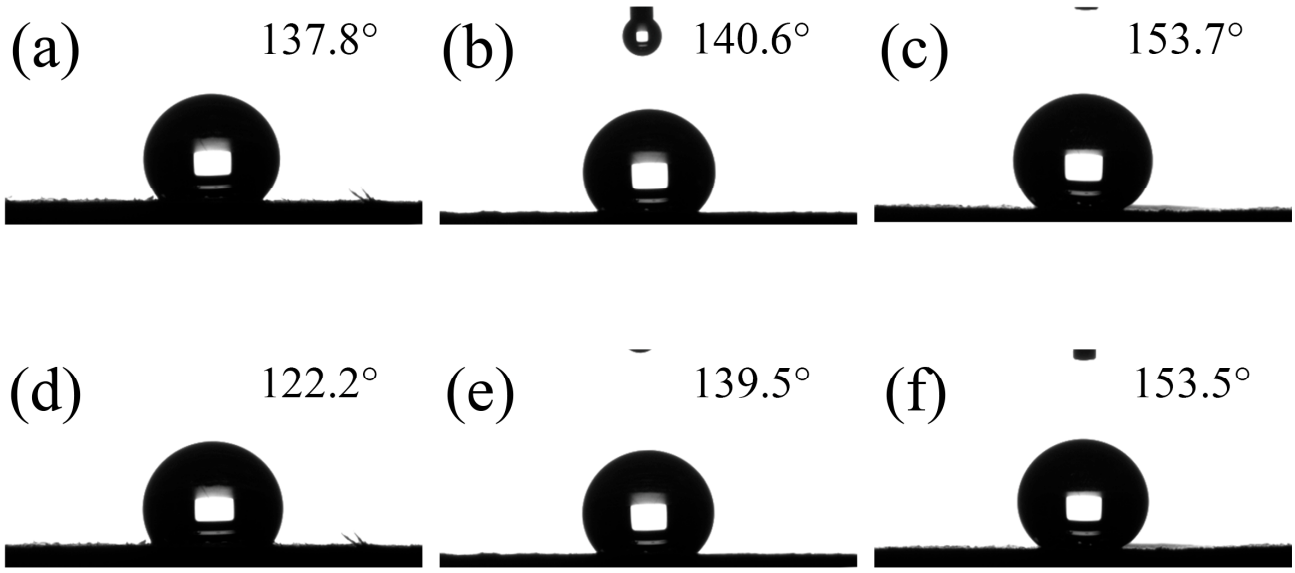

Figure 4. Wettability of the OPA-modified MIL-88(Fe) coated wood surface; (**a**–**c**) are shapes of water droplets after 10 s holding for wood surface, MIL-88(Fe)-coated wood surface with 5.0×10^{-2} M and 10.0×10^{-2} M reactants' concentration, respectively; (**d**–**f**) are shapes of water droplets stable for wood surface, MIL-88(Fe)-coated wood surface with 5.0×10^{-2} M and 10.0×10^{-2} M reactants' concentration, respectively.

3.5. Discussion

Based on the results of the characterization described above, it can be demonstrated that incorporating MIL-88(Fe) into wood surfaces can enhance their hydrophobic properties. The higher the density of MIL-88(Fe) adhered to the wood surface, the better the hydrophobic properties. The theory of the improved hydrophobic performance can be explained by the fact that unmodified wood pieces have a relatively flat surface with few nanostructures, which makes it simple for water droplets to spread out on it. In addition, OPA can combine with wood pieces due to the presence of hydroxyl, carboxyl, and other groups on the surface of wood pieces; however, the binding force is weak, resulting in a low OPA concentration on the surface of wood pieces that easily falls off, as illustrated in Figure 5a. As a result, unmodified wood pieces have a low water contact angle on their surface, making it simple for water droplets to penetrate the wood pieces. Due to the large grain size of MIL-88(Fe), a large nanomastoid structure is generated on the wood pieces surface following OPA@MIL-88(Fe) modification. These grains are not evenly spaced out, and the midsection has a lot of gaps. Second, the MIL-88(Fe) frame structure contains Fe metal sites, and these metal sites create a strong double coordination chemical bond (Fe-O-P) with the groups in OPA [39], securing OPA to the wood surface and orienting its hydrophobic long chain part away from the wood surface (as shown in Figure 5b). Third, MIL-88(Fe) can offer additional metal sites due to its large specific surface. The OPA@MIL-88(Fe)-modified wood surface offers higher hydrophobic characteristics when the three aforementioned elements are combined. The MIL-88(Fe) density on this wood block, however, is low, and some of the wood's surface is not covered with MIL-88(Fe). In addition, the contact angle

is slightly lower since the wood pieces and water are in direct contact, and some water is drawn into the wood pieces. More mastoid structures generated more voids as the density of OPA@MIL-88(Fe) on the wood pieces surface rose, and MIL-88(Fe) offered additional metal sites to bind to OPA, further enhancing the hydrophobic property until it reached the super hydrophobic level. According to the experiment's findings, the hydrophobic properties of MIL-88(Fe) synthesized on wood pieces surfaces should be improved. However, it is confirmed that if the reactant concentration is increased further, 1,4-dicarboxybenzene will not entirely dissolve in DMF.

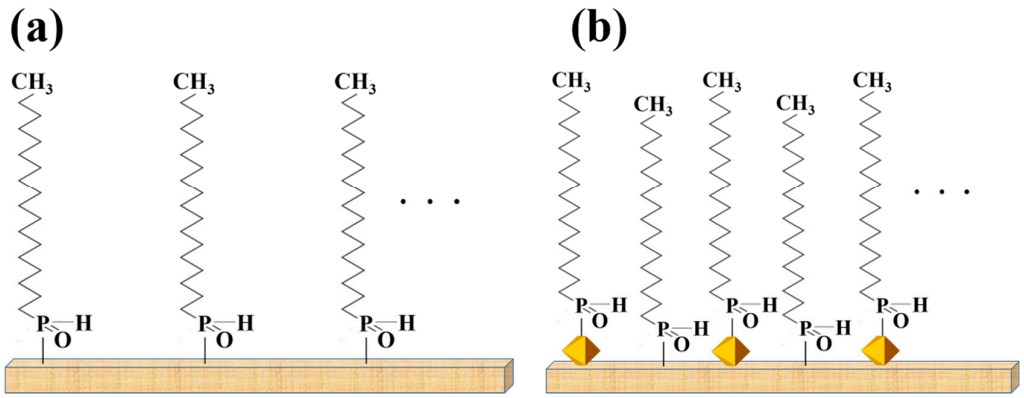

Figure 5. (**a**) Schematic diagram of unmodified poplar wood's surface, (**b**) schematic diagram of OPA@MIL-88(Fe)-modified poplar wood's superhydrophobic surface.

4. Conclusions

In conclusion, the solvothermal method was used to obtain the superhydrophobic wood surface. The process for fabricating a superhydrophobic wood surface involves the creation of nano shuttle MIL-88(Fe) particles, which produce a homogeneous, high-density nano mastoid structure and metal sites on the surface of the wood pieces. Additionally, the wood's surface was modified using n-Octadecylphosphonic acid to retain the long-chain alkane hydrophobic group outward. The findings of this research suggest that a hydrophobic wood pieces surface requires a nano mastoid structure, a high surface area, and low surface free energy. Wood pieces should be protected against rotting, mildew, crazing, and deformation by the superhydrophobic surface, created using the OPA-modified MIL-88(Fe) on the wood pieces. Wood pieces resources' useful lives might be efficiently increased.

Author Contributions: Conceptualization, D.Q.; methodology, Y.H. and P.M.; investigation, Y.H., J.W. and P.M.; writing—original draft preparation, Y.H. and J.W.; writing—review and editing, Y.H. and J.W.; funding acquisition, D.Q. and J.W. All authors have read and agreed to the published version of the manuscript.

Funding: This research was funded by the National Natural Science Foundation of China, grant number 31570712 and Fundamental Research Funds for the Central Universities, grant number 2572020BC02.

Data Availability Statement: There are no shared data available.

Conflicts of Interest: The authors declare no conflict of interest.

References

1. Jiang, F.; Li, T.; Li, Y.; Zhang, Y.; Gong, A.; Dai, J.; Hitz, E.; Luo, W.; Hu, L. Wood-Based Nanotechnologies toward Sustainability. *Adv. Mater.* **2018**, *30*, 1703453. [CrossRef] [PubMed]
2. Huang, W.; Li, H.; Zheng, L.; Lai, X.; Guan, H.; Wei, Y.; Feng, H.; Zeng, X. Superhydrophobic and high-performance wood-based piezoresistive pressure sensors for detecting human motions. *Chem. Eng. J.* **2021**, *426*, 130837. [CrossRef]
3. Yang, H.; Wang, S.; Wang, X.; Chao, W.; Wang, N.; Ding, X.; Liu, F.; Yu, Q.; Yang, T.; Yang, Z.; et al. Wood-based composite phase change materials with self-cleaning superhydrophobic surface for thermal energy storage. *Appl. Energy* **2020**, *261*, 114481. [CrossRef]

4. Barthlott, W.; Neinhuis, C. Purity of the sacred lotus, or escape from contamination in biological surfaces. *Planta* **1997**, *202*, 1–8. [CrossRef]
5. Sun, T.; Feng, L.; Gao, X.; Jiang, L. Bioinspired surfaces with special wettability. *Acc. Chem. Res.* **2005**, *38*, 644–652. [CrossRef]
6. Perumanath, S.; Pillai, R.; Borg, M.K. Contaminant Removal from Nature's Self-Cleaning Surfaces. *Nano Lett.* **2023**, *23*, 4234–4241. [CrossRef] [PubMed]
7. Gan, W.; Gao, L.; Zhang, W.; Li, J.; Zhan, X. Fabrication of microwave absorbing $CoFe_2O_4$ coatings with robust superhydrophobicity on natural wood surfaces. *Ceram. Int.* **2016**, *42*, 13199–13206. [CrossRef]
8. Tu, K.; Wang, X.; Kong, L.; Guan, H. Facile preparation of mechanically durable, self-healing and multifunctional superhydrophobic surfaces on solid wood. *Mater. Des.* **2018**, *140*, 30–36. [CrossRef]
9. Yang, J.; Li, H.; Yi, Z.; Liao, M.; Qin, Z. Stable superhydrophobic wood surface constracting by KH580 and nano-Al_2O_3 on polydopamine coating with two process methods. *Colloids Surf. A Physicochem. Eng. Asp.* **2022**, *637*, 128219. [CrossRef]
10. Yao, Q.; Jin, C.; Zheng, H.; Ma, Z.; Sun, Q. Superhydrophobicity, microwave absorbing property of $NiFe_2O_4$/wood hybrids under harsh conditions. *J. Nanomater.* **2016**, *2015*, 761286. [CrossRef]
11. Łukawski, D.; Lekawa-Raus, A.; Lisiecki, F.; Koziol, K.; Dudkowiak, A. Towards the development of superhydrophobic carbon nanomaterial coatings on wood. *Prog. Org. Coat.* **2018**, *125*, 23–31. [CrossRef]
12. Sun, Q.; Lu, Y.; Liu, Y. Growth of hydrophobic TiO_2 on wood surface using a hydrothermal method. *J. Mater. Sci.* **2011**, *46*, 7706–7712. [CrossRef]
13. Zhang, H.; Li, Y.; Lu, Z.; Chen, L.; Huang, L.; Fan, M. A robust superhydrophobic TiO_2 NPs coated cellulose sponge for highly efficient oil-water separation. *Sci. Rep.* **2017**, *7*, 9428. [CrossRef]
14. Yue, D.; Lin, S.; Cao, M.; Lin, W.; Zhang, X. Fabrication of transparent and durable superhydrophobic polysiloxane/SiO_2 coating on the wood surface. *Cellulose* **2021**, *28*, 3745–3758. [CrossRef]
15. Shupe, T.; Piao, C.; Lucas, C. The termiticidal properties of superhydrophobic wood surfaces treated with ZnO nanorods. *Eur. J. Wood Wood Prod.* **2012**, *70*, 531–535. [CrossRef]
16. Sun, Q.F.; Lu, Y.; Li, J.; Cao, J. Self-Assembly of a Superhydrophobic ZnO Nanorod Arrays Film on Wood Surface Using a Hydrothermal Method. *Key Eng. Mater.* **2014**, *609–610*, 468–471. [CrossRef]
17. Hsieh, C.-T.; Chang, B.-S.; Lin, J.-Y. Improvement of water and oil repellency on wood substrates by using fluorinated silica nanocoating. *Appl. Surf. Sci.* **2011**, *257*, 7997–8002. [CrossRef]
18. Wang, C.; Piao, C.; Lucas, C. Synthesis and characterization of superhydrophobic wood surfaces. *J. Appl. Polym. Sci.* **2011**, *119*, 1667–1672. [CrossRef]
19. Shah, S.M.; Zulfiqar, U.; Hussain, S.Z.; Ahmad, I.; Rehman, H.U.; Hussain, I.; Subhani, T. A durable superhydrophobic coating for the protection of wood materials. *Mater. Lett.* **2017**, *203*, 17–20. [CrossRef]
20. Wang, S.; Liu, C.; Liu, G.; Zhang, M.; Li, J.; Wang, C. Fabrication of superhydrophobic wood surface by a sol–gel process. *Appl. Surf. Sci.* **2011**, *258*, 806–810. [CrossRef]
21. Lu, Q.; Jiang, H.; Cheng, R.; Xia, S.; Zhan, K.; Yi, T.; Morrell, J.J.; Yang, L.; Du, G.; Gao, W. Preparation of superhydrophobic wood surfaces via in-situ synthesis of $Cu_2(OH)_3Cl$ nano-flowers and impregnating PF&STA to improve chemical and mechanical durability. *Ind. Crops Prod.* **2021**, *172*, 113952. [CrossRef]
22. Jayaramulu, K.; Geyer, F.; Schneemann, A.; Kment, Š.; Otyepka, M.; Zboril, R.; Vollmer, D.; Metal-Organic, R.A. Frameworks: Hydrophobic Metal-Organic Frameworks. *Adv. Mater.* **2019**, *31*, 1970230. [CrossRef]
23. Lu, Y.; Wu, Y.; Yang, J.; Zhu, X.; Sun, F.; Li, L.; Shen, Z.; Pang, Y.; Wu, Q.; Chen, H. Gentle fabrication of colorful superhydrophobic bamboo based on metal-organic framework. *J. Colloid Interface Sci.* **2021**, *593*, 41–50. [CrossRef]
24. Ma, D.Y.; Li, Z.; Zhu, J.X.; Zhou, Y.P.; Chen, L.L.; Mai, X.F.; Liufu, M.L.; Wu, Y.B.; Li, Y.W. Inverse and highly selective separation of CO_2/C_2H_2 on a thulium-organic framework. *J. Mater. Chem. A* **2020**, *8*, 11933–11937. [CrossRef]
25. Zhong, Y.Y.; Peng, Z.X.; Peng, Y.Q.; Li, B.; Pan, Y.; Ouyang, Q.; Sakiyama, H.; Muddassir, M.; Liu, J.Q. Construction of Fe-doped ZIF-8/DOX nanocomposites for ferroptosis strategy in the treatment of breast cancer. *J. Mater. Chem. B* **2023**, *11*, 6335–6345. [CrossRef]
26. Chen, X.; Li, M.; Lin, M.; Lu, C.; Kumar, A.; Pan, Y.; Liu, J.-Q.; Peng, Y. Current and promising applications of Hf(iv)-based MOFs in clinical cancer therapy. *J. Mater. Chem. B* **2023**, *11*, 5693–5714. [CrossRef]
27. Ke, F.; Pan, A.; Liu, J.; Liu, X.; Yuan, T.; Zhang, C.; Fu, G.; Peng, C.; Zhu, J.; Wan, X. Hierarchical camellia-like metal–organic frameworks via a bimetal competitive coordination combined with alkaline-assisted strategy for boosting selective fluoride removal from brick tea. *J. Colloid Interface Sci.* **2023**, *642*, 61–68. [CrossRef]
28. Dalapati, R.; Nandi, S.; Gogoi, C.; Shome, A.; Biswas, S. Metal–Organic Framework (MOF) Derived Recyclable, Superhydrophobic Composite of Cotton Fabrics for the Facile Removal of Oil Spills. *ACS Appl. Mater. Interfaces* **2021**, *13*, 8563–8573. [CrossRef]
29. Gao, M.-L.; Zhao, S.-Y.; Chen, Z.-Y.; Liu, L.; Han, Z.-B. Superhydrophobic/Superoleophilic MOF Composites for Oil–Water Separation. *Inorg. Chem.* **2019**, *58*, 2261–2264. [CrossRef]
30. Zhu, X.-W.; Zhou, X.-P.; Li, D. Exceptionally water stable heterometallic gyroidal MOFs: Tuning the porosity and hydrophobicity by doping metal ions. *Chem. Commun.* **2016**, *52*, 6513–6516. [CrossRef]
31. Zango, Z.U.; Jumbri, K.; Sambudi, N.S.; Bakar, N.H.H.A.; Abdullah, N.A.F.; Basheer, C.; Saad, B. Removal of anthracene in water by MIL-88 (Fe), NH_2-MIL-88 (Fe), and mixed-MIL-88 (Fe) metal–organic frameworks. *RSC Adv.* **2019**, *9*, 41490–41501. [CrossRef] [PubMed]

32. Kamperidou, V.; Barboutis, I. Vasileiou, Effect of Thermal Treatment on Colour and Hygroscopic Properties of Poplar Wood. 2012. Available online: https://www.researchgate.net/publication/290945720_Effect_of_thermal_treatment_on_colour_and_hygroscopic_properties_of_poplar_wood (accessed on 12 October 2012).
33. Zhao, M.; Tao, Y.; Wang, J.; He, Y. Facile preparation of superhydrophobic porous wood for continuous oil-water separation. *J. Water Process. Eng.* **2020**, *36*, 101279. [CrossRef]
34. Zhou, Z.; Zhang, Q.; Sun, J.; He, B.; Guo, J.; Li, Q.; Li, C.; Xie, L.; Yao, Y. Metal–Organic Framework Derived Spindle-like Carbon Incorporated α-Fe_2O_3 Grown on Carbon Nanotube Fiber as Anodes for High-Performance Wearable Asymmetric Supercapacitors. *ACS Nano* **2018**, *12*, 9333–9341. [CrossRef]
35. Han, B.; Li, Y.; Qian, B.; He, Y.; Peng, L.; Yu, H. Adsorption and determination of polycyclic aromatic hydrocarbons in water through the aggregation of graphene oxide. *Open Chem.* **2018**, *16*, 716–725. [CrossRef]
36. Chen, X.; Kuwahara, Y.; Mori, K.; Louis, C.; Yamashita, H. Heterometallic and Hydrophobic Metal–Organic Frameworks as Durable Photocatalysts for Boosting Hydrogen Peroxide Production in a Two-Phase System. *ACS Appl. Energy Mater.* **2021**, *4*, 4823–4830. [CrossRef]
37. Chen, X.; Kuwahara, Y.; Mori, K.; Louis, C.; Yamashita, H. A hydrophobic titanium doped zirconium-based metal organic framework for photocatalytic hydrogen peroxide production in a two-phase system. *J. Mater. Chem. A* **2020**, *8*, 1904–1910. [CrossRef]
38. Kawase, Y.; Isaka, Y.; Kuwahara, Y.; Mori, K.; Yamashita, H. Ti cluster-alkylated hydrophobic MOFs for photocatalytic production of hydrogen peroxide in two-phase systems. *Chem. Commun.* **2019**, *55*, 6743–6746. [CrossRef]
39. Sun, Y.; Sun, Q.; Huang, H.; Aguila, B.; Niu, Z.; Perman, J.A.; Ma, S. A molecular-level superhydrophobic external surface to improve the stability of metal–organic frameworks. *J. Mater. Chem. A* **2017**, *5*, 18770–18776. [CrossRef]